

Received March 3, 2019, accepted March 16, 2019, date of current version April 10, 2019.

Digital Object Identifier 10.1109/ACCESS.2019.2908001

Mutual Coupling Reduction Using Hybrid Technique in Wideband Circularly Polarized MIMO Antenna for WiMAX Applications

JAVED IQBAL¹, USMAN ILLAHI¹, MOHAMAD ISMAIL SULAIMAN¹,
MUHAMMAD MANSOOR ALAM^{2,3}, MAZLIHAM MOHD SU'UD⁴,
AND MOHD NAJIB MOHD YASIN⁵

¹British Malaysian Institute (BMI), Universiti Kuala Lumpur, Gombak 53100, Malaysia

²Institute of Business and Management (IoBM), Karachi 74900, Pakistan

³Malaysian Institute of Information Technology (MIIT), Universiti Kuala Lumpur, Kuala Lumpur 50250, Malaysia

⁴Universiti Kuala Lumpur, Kuala Lumpur 50250, Malaysia

⁵School of Microelectronic Engineering, Bioelectromagnetics Research Group, Universiti Malaysia Perlis, Arau, Malaysia

Corresponding author: Mohamad Ismail Sulaiman (mismail@unikl.edu.my)

This work was supported by the Universiti Kuala Lumpur, Malaysia, through the Short Term Research Grant (STRG).

ABSTRACT In this paper, a novel wideband circularly polarized multiple-input multiple-output (MIMO) dielectric resonator antenna (DRA) has been proposed for worldwide interoperability for microwave access (WiMAX) applications. The mutual coupling (MC) between closely placed DRA units at 0.5λ has been significantly reduced by using a new hybrid technique. The exclusive features of the proposed MIMO antenna include wide impedance matching bandwidth (BW), broadband circular polarization (CP), and suppressed MC between the radiating elements. The first step of hybrid technique is the employment of parasitic patch at an optimized distance beside the conformal metal strip of the two identical rectangular DRAs in order to generate CP wave along with a wide impedance matching BW over the same frequency range. In the final step, the MC is suppressed significantly along with the broadband CP by placing the DRAs diagonally at an optimized position. The proposed MIMO antenna is the hybrid of the parasitic patch and the diagonal position of radiating elements. The CP BW offered by the proposed antenna is $\sim 20.82\%$ (3.58–4.40 GHz) in conjunction with an impedance-matching BW of $\sim 38.51\%$ (3.50–4.95 GHz). Moreover, MC less than -28 dB is achieved over the entire band and -26 dB at 3.89 GHz (minimum of the AR) through the hybrid technique. The prototype of the proposed antenna geometry is fabricated and measured. A good agreement has been attained between the simulated and measured results.

INDEX TERMS MIMO antenna, DRA, parasitic patch, CP, conformal strip.

I. INTRODUCTION

Over a recent couple of decade, dielectric resonator antennas (DRAs) attained the attention of researchers worldwide due to the features such as high gain, temperature stability, high radiation efficiency specially for higher frequencies due to low ohmic losses [1]. As compared to microstrip patch antenna DRA proves to be a better alternative in term of gain, CP and impedance BW [2].

Inherently DRA possesses properties of wider BW if low permittivity material is utilized. Additionally, The size of the DRA is proportional to $\lambda_0/\sqrt{\epsilon_r}$ where $\lambda_0 = c/f_0$ due to

The associate editor coordinating the review of this manuscript and approving it for publication was Hayder Al-Hraishawi.

this, the BW enhancement and miniaturization of the antenna cannot be achieved at the same time [3] and [4]. In [5]–[7], wider BW has been reported using perforated or fractural DRA, however, these approaches make the design more complicated and fragile. Moreover, the precise cutting of perforated DRA is a challenging task. This issue can be resolved by using the parasitic patch without compromising on the DRA size and shape. In the recent years, tremendous efforts have been paid on wideband impedance matching and CP bandwidths. As circular polarized systems are insensitive to the orientation of the transmitting and receiving antennas so it can be utilized in various wireless applications. Many researchers have attempted to attain CP by utilizing quadrature and dual

feeding [8] methods but it has the limitation like increasing in complexity of the antenna design and size.

An alternative approach to generate CP is through the parasitic patch. The use of a parasitic patch was first introduced by [9] and later by [10] on the DRA. Approximately 116.7% impedance bandwidth has been achieved by the use of a parasitic patch at the bottom of stacked fractal tetrahedron shaped DRA, but the antenna is linearly polarized [5]. As reported in [11], where very narrow BW of 2.4% is obtained by placing the parasitic patch on hemispherical DRA. In [12] excitation of chamfered rectangular DRA using probe feed with parasitic patch reported a 3-dB AR BW of $\sim 10.06\%$. CP bandwidth of 11.5% is achieved by placing the parasitic patch at an optimized distance beside cylindrical DRA feed [13]. Furthermore, CP of $\sim 2.5\%$ is attained in [14] by placing the parasitic patch on top of Rectangular DRA. In this design [15] strip is loading on the top of cylindrical DRA; the antenna provides AR over a BW of 3.14% below 3-dB for CP. Two orthogonal degenerated modes are generated by employing the DR element on the edge of the circular microstrip patch antenna. The CP radiation exhibits an AR bandwidth of 3.7% (2.39–2.48 GHz) [16]. In this CP design [17] a parasitic patch is attached near a corner of the DRA to generate circularly polarized fields. The said design provides a 3-dB bandwidth of 11.8%, which is ~ 3 times of original design. Over a couple of decades, a significant progress in wireless activities has boosted the MIMO antenna technologies. For the wireless application, MIMO antenna systems are used for long-term evolution (LTE) network, wireless local area network (WLAN), and worldwide interoperability for microwave access (WiMAX). MIMO system offers a better quality of services in non-line of sight (NLOS) communication since it offers significantly wider BW of up to hundreds of gigabit compared to a single input single-output (SISO) system [18]. Additionally, MIMO antennas have the capability to improve the channel capacity over a limited available BW to attain a high data rate. One of the main criteria to design the MIMO antenna system is having low MC among the radiating elements of an array. Highly efficient MIMO antenna cannot be designed through patch antenna because of less radiation efficiency [19]. As DRA possess high radiation efficiency and it's not even degraded in the array configuration. So, DRA is much more preferable choice of the researcher for MIMO applications.

A great deal of work has been reported in the literature on reducing MC between the DRA elements. In [20] by using electromagnetic bandgap (EBG) structure ~ 13 dB isolation is achieved over desire frequency range however EBG make the design more complicated. While on the other, side split ring resonator (SRR) has been used [21] to reduce MC at higher frequency i.e. 60GHz However, the gain radiation pattern is not appropriate in the desired frequency range. Isolation among the antenna radiators enhanced up to ~ 15 dB, by using fractal DRA in [3] but the cutting of DRA is very challenging. As one of the basic reasons for MC between the antennas is propagating through

surface waves, that can we overcome by incorporating defected ground structure (DGS) between the cylindrical DRAs [7]. significantly MC reduces i.e. ~ 16 dB by using metamaterial polarization-rotator wall (MPR) between the cylindrical DRA [22], nevertheless, all the above mentioned MIMO antennas are linearly polarized and in case of antenna misalignment, antenna performance degrade dramatically [23]. Most of the researcher focus on MIMO patch antennas and proposed different techniques to reduce MC but in parallel, no significant work has been done yet on MIMO DRAs especially circularly polarized antennas except few are accounted in the literature [23]–[27] to overcome the issues of misalignment.

In this communication, a broadband circularly polarized DRA MIMO antenna is proposed as it offers low MC ($|S_{21}/S_{12}| < -28$ dB) between the DRAs having wider impedance and the CP BWs of $\sim 38.5\%$ and $\sim 20.82\%$ respectively. Along with this high diversity gain (DG) and low envelope correlation coefficient (ECC) is observed. The proposed antenna operates over a wide frequency range of 3.50–4.95 GHz suitable for WiMAX [28].

This manuscript is organized as follow. Section II gives the configuration of the single antenna element, followed by transaction to proposed antenna array design, the operating principle, BW enhancement, generating CP and discussion on simulation results. Measurement results of prototype are discussed in Section III. Finally, the conclusions are drawn in Section IV.

II. ANTENNA CHARACTERIZATION

In this section, geometry of the single element along with dimension and working mechanisms and simulated results are explained.

A. SINGLE ELEMENT OF MIMO ANTENNA

Fig. 1 illustrates a rectangular DRA excited by E-shaped conformal metal strip. Presently, conformal metal strip can be used to replace conventional probe feed, Other feeding mechanisms like coaxial feed having air gap issue which in leads to frequency deviation [13], that is easily overcome in a conformal feed. Furthermore, the conformal strip has been used for good impedance matching as it couples energy from source to DRA very efficiently [3]. The conformal metal feeding strips were made up of conducting adhesive copper tape which easily sticks to the DRA walls. The novel E-shaped conformal feed consists of seven individually cut strips.

After running the parametric sweep, the optimized feed parameters were found to be $H_1 = 1_2$ mm, b_2 and $b_4 = 7.0$ mm, $b_3 = 9.0$ mm, and lengths l_2 and $l_4 = 3.5$ mm, $l_3 = 5.0$ mm and distance between feed and DRA edge is $b_1 = 8.0$ mm. The width of all the strips are optimized at 1mm except w_1 i.e. 2mm. The dimension of the rectangular DRA is taken from [8] where, $H = 26.1$ mm, $B = 25.4$ mm, and $C = 14.3$ mm. The DRA is made up of ECCO-STOCK HIK material having relative permittivity $\epsilon_r = 10$.

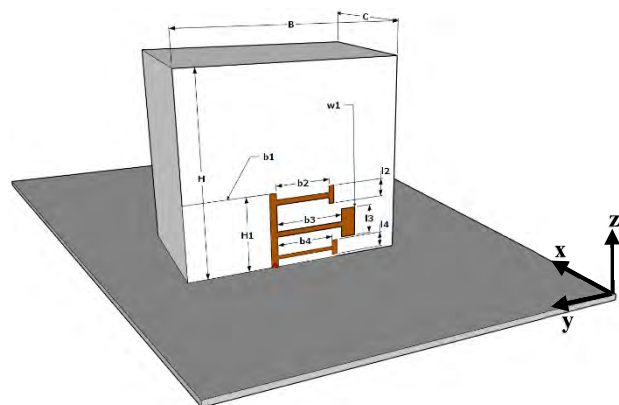


FIGURE 1. Geometry of the linearly polarized single element.

The parametric and simulated results are carried out in commercially available software i.e. computer simulation technology (CST-2017).

E-shaped conformal metal strip of single unit provide simulated reflection coefficient (S_{11}) bandwidth of $\sim 7.85\%$, covering the frequency range from 3.61-3.91GHz and gain of $\sim 5.2\text{dBi}$ over the same frequency range as shown in Fig. 2. As single unit only excite the fundamental mode with in the DRA therefore the design is said to be linearly polarized and hence no axial ratio is attained.

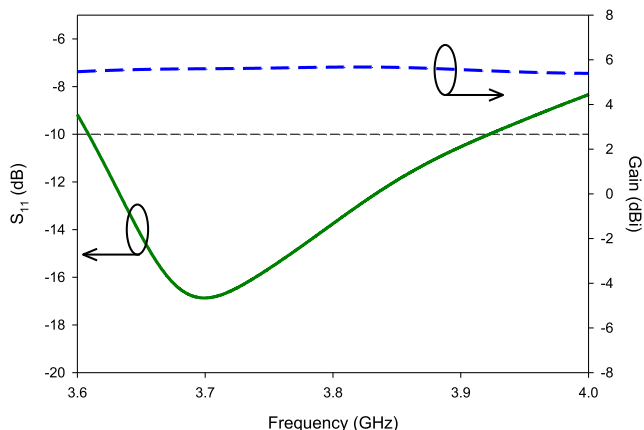


FIGURE 2. Simulated S-parameter and Gain of the single unit.

B. LINEARLY POLARIZED MIMO ANTENNA

In this subsection, the geometry and dimensions of the linearly polarized MIMO-antenna is shown in Fig. 3 (a). The two radiating elements are placed on an aluminum ground plane of size $35 \times 35 \text{ cm}^2$. The edge-to-edge spacing (d) between the radiating element is $\lambda_0/2$, where λ_0 is the wavelength with respect to the lowest frequency of operation i.e. 3.722 GHz, the feed of the proposed DRA has been excited through discrete edge port in CST-2017 simulator. Fig. 4 shows the design evolution phases, in the 1st stage, as obvious, antenna-1 is an array of single unit, that has been designed and simulated for the desired results, in 2nd stage

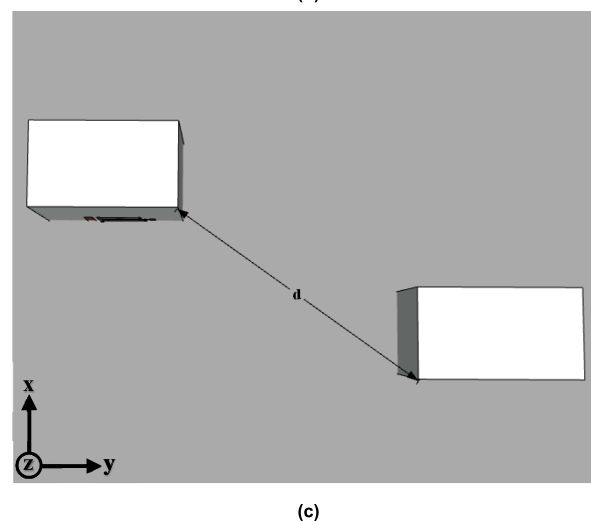
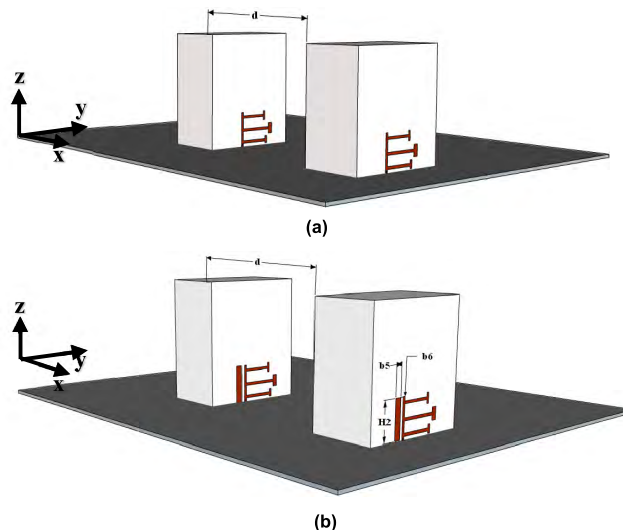


FIGURE 3. Transition from linearly polarized to proposed wideband circularly polarized MIMO antenna (a) Antenna-1 (b) Antenna-2 (c) Proposed Antenna (Top View).

parasitic patch has been introduced as shown in antenna-2, at an optimized distance to the E-shaped conformal metal strip i.e., $b_6 = 0.5 \text{ mm}$. The optimized dimensions of the parasitic patch are $H_2 = 11.50 \text{ mm}$ and width $b_5 = 2\text{mm}$. In the last and 3rd step hybrid (parasitic patch and diagonal position) technique has been introduced, which leads to the final design of DRA. In all the stages the edge-to-edge spacing (d) between the radiating elements is kept at $\lambda_0/2$.

Simulated reflection coefficient (S_{11}) and transmission coefficient (S_{12}) of all the three stages are depicted in Fig. 4. The AR (3-dB) of antenna-2 and proposed MIMO is demonstrated in Fig. 6. High MC and narrow impedance BW is always undesirable in high-performance MIMO antennas and this is what illustrated in simulated results of antenna-1, where a narrow S_{11} BW of 6.27% (3.62–3.84 GHz) and high MC of -15dB have been obtained. The E-shaped feed only excites the single fundamental mode ($TE_{1\delta 1}^y$) inside the DRA, whereas for the generation of CP waves, it is required to excite

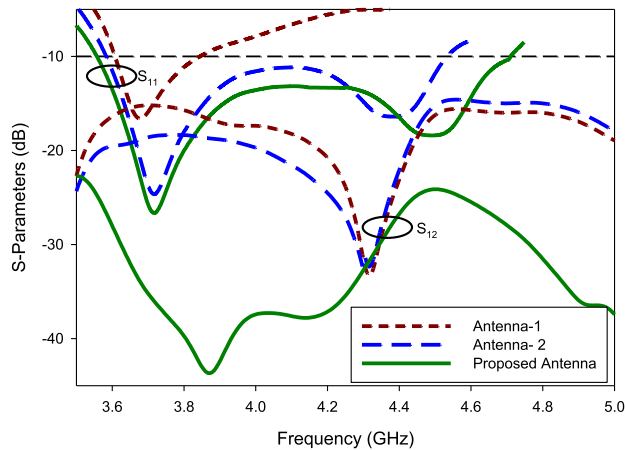


FIGURE 4. Simulated S-parameters to illustrate the effect of change in design.

two orthogonal modes with quadrature phase shift between them.

C. CIRCULARLY POLARIZED MIMO ANTENNA

The antenna-2 has been designed by doing modifications in antenna-1. CP has been achieved by incorporating a parasitic patch as shown in Fig. 3 (b). The degenerate mode pair $TE_{\delta 13}^x$ at 3.74 GHz and $TE_{1\delta 3}^y$ at 4.4 GHz has been excited to generate circularly polarized wave. The simulated distributions of electric field have been shown in Fig. 5. The simulated mode frequencies are quite similar to those predicted by dielectric waveguide model (DWM) [8] i.e. $TE_{\delta 13}^x$ and $TE_{1\delta 3}^y$ at 3.8GHz and 4.53 GHz respectively. For the generation of CP waves, the first condition of orthogonal modes is satisfied, additionally, the minimum of CP of antenna-2 i.e. 3.90 GHz is in between the degenerated modes, thus both conditions for the generation of CP satisfied [13] and [28]. Moreover, the S_{11} BW, has been improved significantly, as the parasitic patches help in achieving additional resonant frequency which in turn lead to wider bandwidth [5]. The simulated reflection coefficient $|S_{11} \leq -10dB|$ bandwidth of $\sim 30.12\%$ and CP bandwidth of $\sim 6.01\%$ have been achieved as shown in Fig.4 and Fig.6 respectively.

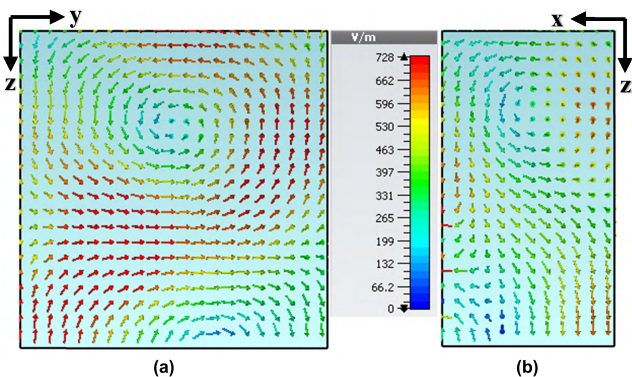


FIGURE 5. Distribution of electric field (a) $TE_{\delta 13}^x$ at 3.74GHz (b) $TE_{1\delta 3}^y$ at 4.4GHz.

High MC in low frequency band is due to the surface waves coupling between feed elements [3] and based on the simulated result, it can be seen that surface wave coupling is more significant in low frequencies (3.55–4.1GHz) of antenna-1 and 2. However, the CP bandwidth and isolation between the radiating elements need to be improved further that is achieved in the proposed design.

D. PROPOSED WIDEBAND CIRCULARLY POLARIZED MIMO ANTENNA

The proposed design of the wideband circularly polarized MIMO antenna has been illustrated in Fig. 7. The final geometry has been proposed on the basis of wide CP bandwidth and enhanced isolation. The design has been achieved by proper positioning of radiating elements as depicted in Fig. 3 (c). Rigorous parametric analysis has been carried out to obtain optimized DRA position. This optimized positioning of DRAs reduce MC throughout the entire band and a broadband CP is achieved. As depicted from Fig. 4, a suitable isolation by more than -28 dB is achieved on average (12 dB at 3.65 GHz, 26 dB at 3.89 GHz, 16 dB at 4.85 GHz). And a significantly wide CP BW of $\sim 21.23\%$ is provided as shown in Fig. 7. The entire AR bandwidth completely falls within the simulated impedance-matching BW of $\sim 34.51\%$ (3.61–4.65 GHz).

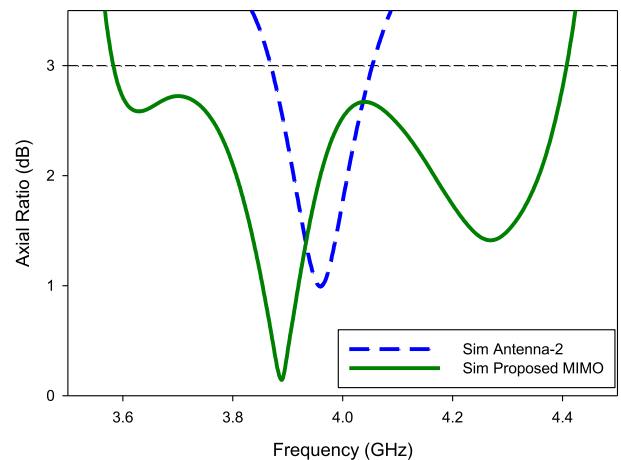


FIGURE 6. Simulated Axial Ratio to illustrate the effect of change in design.

In order to further analyze the performance of wideband circularly polarized MIMO antenna by plotting surface current distribution on the E-shaped conformal strip at a minimum of AR i.e. 3.89 GHz of all 3 modified antennas as presented in Fig. 8. In antenna-1, when port-1 is excited high MC is observed between the DRAs as high current is coupled to the other DRA. To reduce the MC, a parasitic patch is incorporated although this step reduces MC a bit as provided by antenna-2. By positioning the DRAs at optimized diagonal location, the isolation enhanced dramatically and because of this very less amount of current is coupled to the other radiator this is obvious from the Fig. 8.

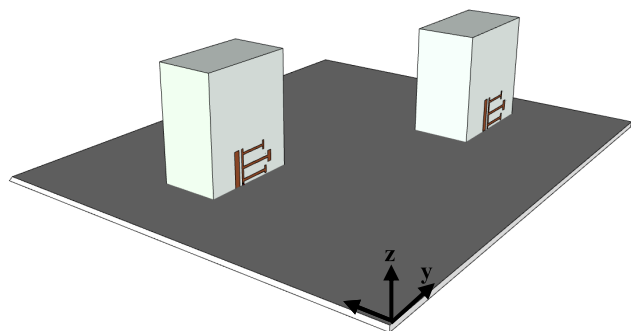


FIGURE 7. Geometry of proposed Wideband Circularly Polarized-MIMO antenna.

TABLE 1. Comparison with other mimo antennas.

Literature	Shape of radiating elements	Isolation technique	BW (GHz)	Isolation (dB)
Ref.[6]	Fractal DRAs	DGS and Sliding	3.89–10.4	>15
Ref.[7]	Fractal DRAs	DGS and Sliding	83.6–12.6	>18
Ref.[21]	Cylindrical DRAs	SRR and Metasurface shield	56.6–64.5	>28
Ref.[22]	Rectangular DRAs	MPR	5.10–5.80	>16
Proposed Antenna	Rectangular DRAs	Parasitic patch and diagonally positioned	3.58–4.40	>28

TABLE 2. Comparison with other MIMO antennas on basis of CP.

Literature	Antenna type	3-dB axial ratio BW (%)	3-dB axial ratio frequency range (GHz)
Ref.[23]	DRAs	13.23	5.15–5.88
Ref.[24]	DRAs	3.50	5.60–5.80
Ref.[25]	Hybrid	3.55	5.55–5.75
Ref.[26]	Printed	1.03	5.77–5.83
Ref.[27]	Hybrid	4.18	5.62–5.86
Proposed Antenna	DRAs	20.82	3.58–4.40

Furthermore, Table-1 compares the performances of proposed antenna w.r.t the previous work on the basis of technique, BW (S_{11}), isolation and CP. In parallel comparison of 3-dB AR performance between different circular polarization generated by MIMO antennas are given in Table-2.

III. RESULTS AND DISCUSSION

The wideband circularly polarized-MIMO antenna is designed by using rectangular DRA. Both the elements are made up of ECCOSTOCK HIK material having dielectric constant $\epsilon_r = 10$. Radiators are placing on the aluminum

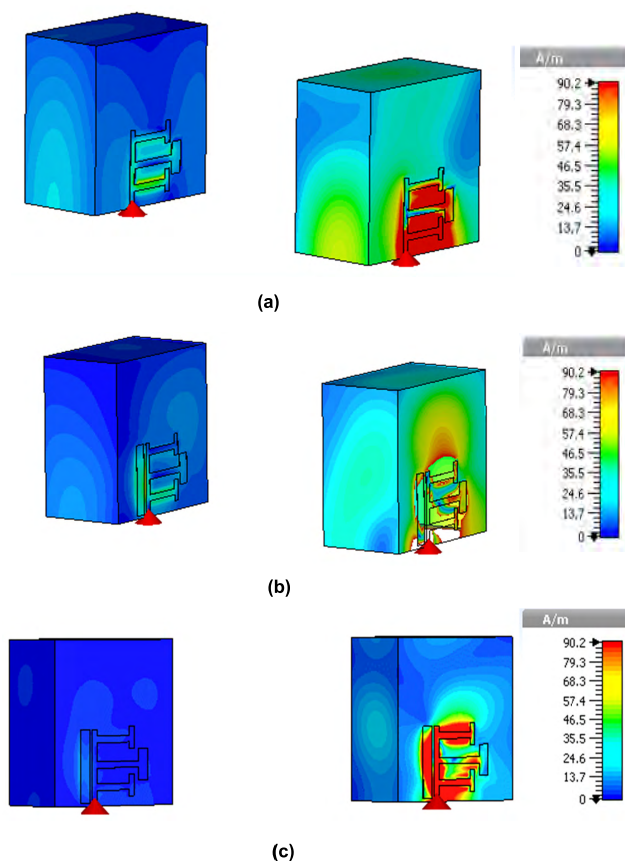
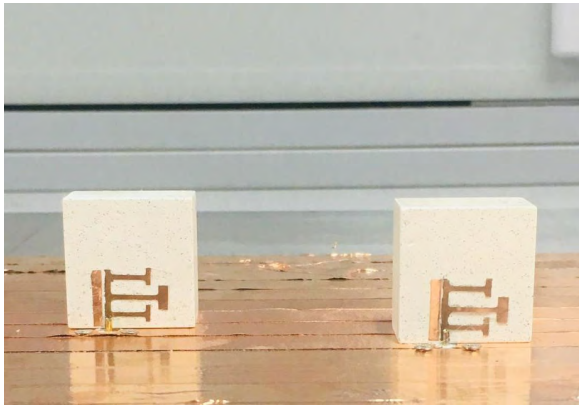


FIGURE 8. Surface Current distribution for (a) Antenna-1, (b) Antenna-2 and (c) proposed antenna.

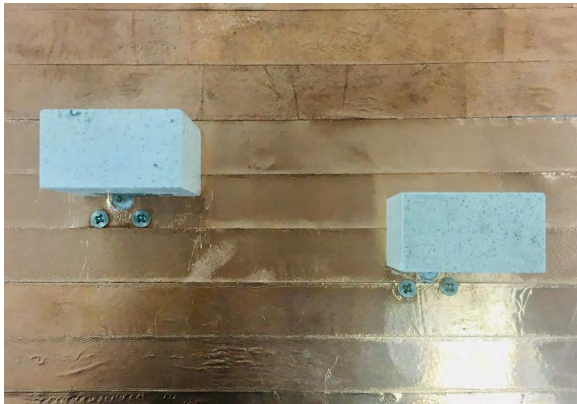
ground plane of $35 \times 35 \text{ cm}^2$. on the other side for simulation and optimization commercially available software CST-2017 is used. For fabrication purpose conformal strip made up of cutting the copper adhesive tape and solder to the inner conductor of SMA connector. Each Antenna is fed by the respective 50Ω coaxial probe. Measurements of the radiation performance of the Far-field parameters (3-dB AR, Gain and radiation pattern) were attained using a Satimo Start Lab System.

A. RETURN LOSSES

Fig. 10 demonstrate simulated and measured reflection coefficients of the prototype. The reflection coefficient was measured using an 8722ES agilent network analyzer (VNA) in an open air condition where simulated results are validated through measured results. Proposed antenna cover wide impedance BW $S_{11}/ S_{22} < -10 \text{ dB}$ of $\sim 38.51\%$ that is achieved over the frequency band of 3.5–4.95 GHz. Measured MC $S_{21}/ S_{12} < -28 \text{ dB}$ is achieved over the entire band. good agreement is attained between the simulation and measurement, and the small discrepancy is mainly caused by the experimental imperfections and fabrication errors. There are two modes visible in S_{11} (simulated and measured) graph, these modes are because of introducing a parasitic patch to the E-shaped conformal strip at an optimized distance.



(a)



(b)

FIGURE 9. Photograph of fabricated circularly polarized wideband MIMO-antenna (a) Front View (b) Top View.

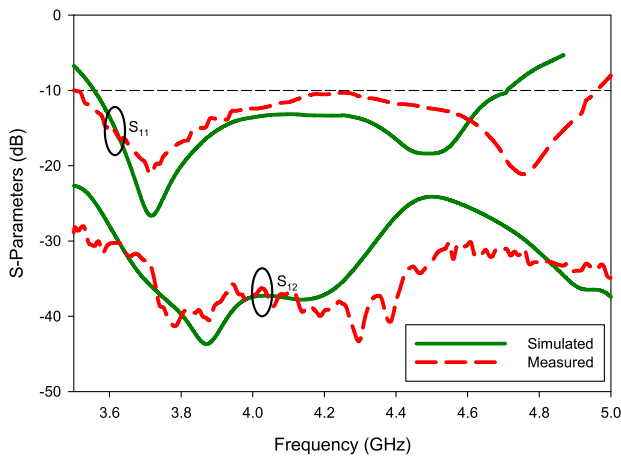


FIGURE 10. S-parameters of the circularly polarized wideband MIMO-antenna.

B. AXIAL RATIO

AR of the proposed design is computed and measured as shown in Fig. 11. From the measured results, it is clear that the diagonally positioned DRAs offers a wide impedance BW of ~21.23%. CP of the MIMO antenna is in conjunction with in impedance matching BW of ~38.51%. Fig. 11 The tested results are closely concurrence with the simulated results.

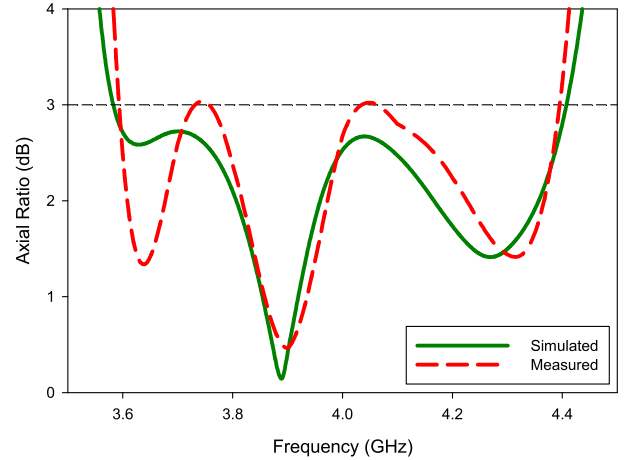


FIGURE 11. Axial ratio of the circularly polarized wideband MIMO antenna.

C. DIVERSITY ANALYSIS

The performance and capabilities of the MIMO antenna are endorsed through envelope correlation coefficient (ECC), in ideal case ECC should be zero [29], but practically limit for better ECC is < 0.5. The formula to calculate ECC using S-parameters is

$$\rho_e = \frac{|S_{11}S_{12} + S_{21}S_{22}|^2}{(1 - |S_{11}|^2 - |S_{21}|^2)(1 - |S_{22}|^2 - |S_{12}|^2)} \quad (1)$$

ECC can be computed by using far-field radiation patterns with the help of Equation (2)

$$\rho_e = \frac{|\iint_{4\pi} [\vec{F}_1(\theta, \phi) \cdot \vec{F}_2(\theta, \phi)] d\Omega|^2}{\iint_{4\pi} |\vec{F}_1(\theta, \phi)|^2 d\Omega \iint_{4\pi} |\vec{F}_2(\theta, \phi)|^2 d\Omega} \quad (2)$$

It is clear from Fig. 12 that measured ECC for the proposed wideband circularly polarized MIMO antenna has < 0.04 for the entire band.

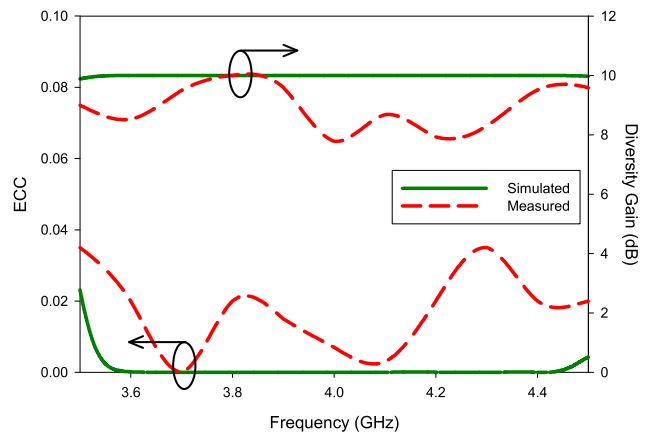


FIGURE 12. ECC and diversity gain of the circularly polarized wideband MIMO antenna.

DG is another parameter to validate the performance of the MIMO antenna. Ideally, the value of DG is 10 but practically

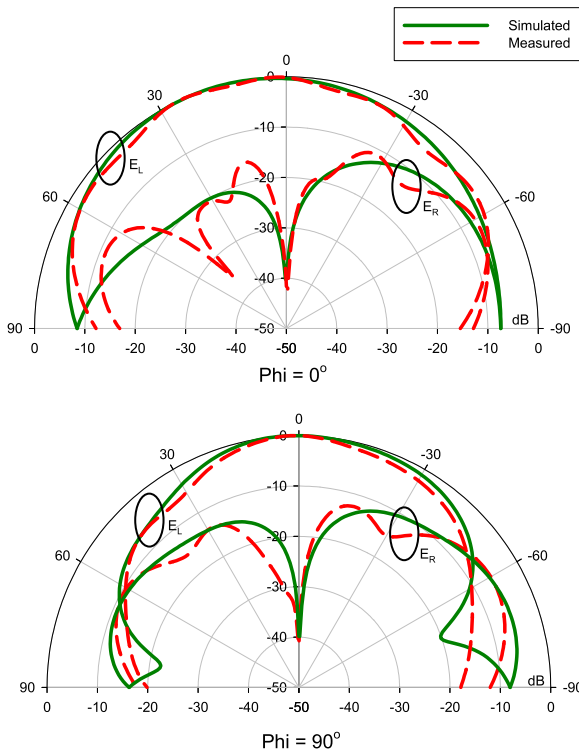


FIGURE 13. Radiation patterns at 3.89 GHz of the circularly polarized wideband MIMO antenna.

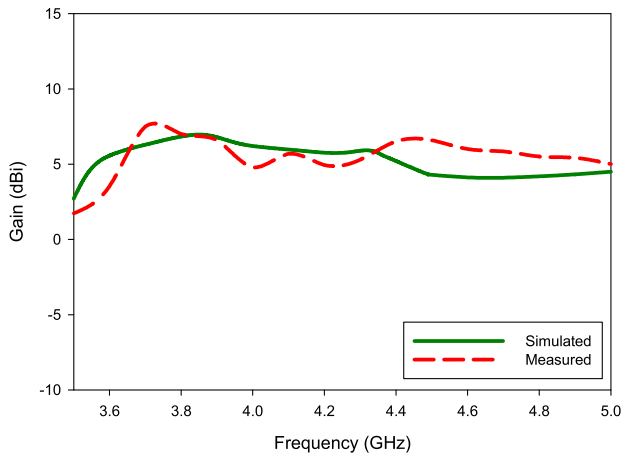


FIGURE 14. Gain of the circularly polarized wideband MIMO antenna.

more than 6 is considered good [29], the value of measured DG for the proposed wideband CP-MIMO antenna is greater than 8 dB as shown in Fig. 12. Following relation can be used to calculate the DG of the MIMO antenna.

$$DG = 10\sqrt{1 - \rho_e^2} \quad (3)$$

D. RADIATION PATTERNS AND GAIN

Fig. 13. depicts the simulated and measured tested 2D radiation patterns at 3.89 GHz (minimum of AR frequency). The left-hand CP (LHCP) and right-hand CP (RHCP) tested patterns are plotted. It is evicted that in both $\phi = 0^\circ$ and $\phi = 90^\circ$ planes, LHCP-radiated fields are dominated over

RHCP fields by >25 dB. On the other side, the tested gain of a proposed antenna is calculated by taking a standard high gain broadband horn antenna (LB-10180) as a reference antenna.

From Fig. 14 simulated and measured gain offered by the proposed antenna is 6.5 dBi and ~6.2 dBi respectively across the whole CP BW

IV. CONCLUSION

Wideband circularly polarized DRA-MIMO antenna has been studied in this article, isolation between the radiators are enhanced by introducing the parasitic patch and further by incorporating the diagonally position of DRAs. CP achieved due to the parasitic patch which in result not only wide the impedance matching BW but also responsible for the degeneration of two orthogonal modes ($TE_{\delta 13}^x$ and $TE_{1\delta 3}^y$).

An important diversity performance parameter for MIMO antenna like diversity and DG results are found to be in an acceptable limit. moreover, the proposed antenna is fabricated and tested, simulated scattering parameters agree well with the measured scattering parameter. The antenna may find its use in WiMAX application.

REFERENCES

- [1] W. M. Abdel-Wahab, M. Abdallah, J. Anderson, Y. Wang, H. Al-Saedi, and S. Safavi-Naeini, "SIW-integrated parasitic DRA array: Analysis, design, and measurement," *IEEE Antennas Wireless Propag. Lett.*, vol. 18, no. 1, pp. 69–73, Jan. 2019.
- [2] R. Chair, A. A. Kishk, and K.-F. Lee, "Comparative study on the mutual coupling between different sized cylindrical dielectric resonator antennas and circular microstrip patch antennas," *IEEE Trans. Antennas Propag.*, vol. 53, no. 3, pp. 1011–1019, Mar. 2005.
- [3] K. Trivedi and D. Pujara, "Mutual coupling reduction in wideband tree shaped fractal dielectric resonator antenna array using defected ground structure for MIMO applications," *Microw. Opt. Technol. Lett.*, vol. 59, no. 11, pp. 2735–2742, Nov. 2017.
- [4] S. Keyrouz and D. Caratelli, "Dielectric resonator antennas: Basic concepts, design guidelines, and recent developments at millimeter-wave frequencies" *Int. J. Antennas Propag.*, vol. 2016, Sep. 2016, Art. no. 6075680.
- [5] K. Trivedi and D. Pujara, "Stacked fractal tetrahedron shaped dielectric resonator antenna for UWB applications," in *Proc. IEEE Appl. Electromagn. Conf. (AEMC)*, Dec. 2017, pp. 1–2.
- [6] K. Trivedi and D. Pujara, "Suppression of mutual coupling in wideband tree shaped fractal DRA array for MIMO applications," in *Proc. 11th Eur. Conf. Antennas Propag. (EUCAP)*, Mar. 2017, pp. 2209–2211.
- [7] K. Trivedi and D. Pujara, "Mutual coupling reduction in UWB modified maltese shaped DRA array for MIMO applications," in *Proc. 48th Eur. Microw. Conf. (EuMC)*, Sep. 2018, pp. 1117–1120.
- [8] B. Li and K. W. Leung, "Strip-fed rectangular dielectric resonator antennas with/without a parasitic patch," *IEEE Trans. Antennas Propag.*, vol. 53, no. 7, pp. 2200–2207, Jul. 2005.
- [9] Z. Li, C. Wu, and J. Litva, "Adjustable frequency dielectric resonator antenna," *Electron. Lett.*, vol. 32, no. 7, pp. 606–607, Mar. 2016.
- [10] Z.-N. Chen, K.-W. Leung, K.-M. Luk, and E. K.-N. Yung, "Effect of parasitic disk on a coaxial probe-fed dielectric resonator antenna," *Microw. Opt. Technol. Lett.*, vol. 15, no. 3, pp. 166–168, Jun. 1997.
- [11] K. W. Leung and H. K. Ng, "Theory and experiment of circularly polarized dielectric resonator antenna with a parasitic patch," *IEEE Trans. Antennas Propag.*, vol. 51, no. 3, pp. 405–412, Mar. 2003.
- [12] M. Abedian, S. K. A. Rahim, S. Danesh, M. H. Jamaluddin, and M. T. Islam, "Compact wideband circularly polarised dielectric resonator antenna," *Electron. Lett.*, vol. 53, no. 1, pp. 5–6, Jan. 2016.
- [13] R. T. Long, R. J. Dorris, S. A. Long, M. A. Khayat, and J. T. Williams, "Use of parasitic strip to produce circular polarisation and increased bandwidth for cylindrical dielectric resonator antenna," *Electron. Lett.*, vol. 37, no. 7, pp. 406–408, Feb. 2001.

- [14] R. Kumari and R. K. Gangwar, "Circularly polarized dielectric resonator antennas: Design and developments," *Wireless Pers. Commun.*, vol. 86, no. 2, pp. 851–886, Jan. 2016.
- [15] A. V. P. Kumar, V. Hamsakutty, J. Yohannan, and K. T. Mathew, "A strip loaded dielectric resonator antenna for circular polarisation," *Microw. Opt. Technol. Lett.*, vol. 48, no. 7, pp. 1354–1356, Jul. 2006.
- [16] C.-L. Tsai, S.-M. Deng, T.-W. Chen, and L.-W. Liu, "Circularly polarized dielectric resonator-loaded circular microstrip patch antennas for WLAN 2.4 GHz applications," *Microw. Opt. Technol. Lett.*, vol. 51, no. 6, pp. 1470–1473, Jun. 2009.
- [17] K. Lu and K. W. Leung, "Wideband circularly polarized hollow dielectric resonator antenna with a parasitic strip," in *Proc. Cross Strait Quad-Regional Radio Sci. Wireless Technol. Conf.*, vol. 1, Jul. 2011, pp. 514–515.
- [18] A. Toktas and A. Akdagli, "Wideband MIMO antenna with enhanced isolation for LTE, WiMAX and WLAN mobile handsets," *Electron. Lett.*, vol. 50, no. 10, pp. 723–724, May 2014.
- [19] M. S. Sharawi, A. B. Numan, and D. N. Aloji, "Isolation improvement in a dual-band dual-element MIMO antenna system using capacitively loaded loops," *Prog. Electromagn. Res.*, vol. 134, pp. 247–266, Feb. 2013.
- [20] M. J. Al-Hasan, T. A. Denidni, and A. R. Sebak, "Millimeter-wave compact EBG structure for mutual coupling reduction applications," *IEEE Trans. Antennas Propag.*, vol. 63, no. 2, pp. 823–828, Feb. 2015.
- [21] A. Dadgarpour, B. Zarghooni, B. S. Virdee, T. A. Denidni, and A. A. Kishk, "Mutual coupling reduction in dielectric resonator antennas using metasurface shield for 60-GHz MIMO systems," *IEEE Antennas Wireless Propag. Lett.*, vol. 16, pp. 477–480, 2017.
- [22] M. Farahani, J. Pourahmadazar, M. Akbari, M. Nedil, A. R. Sebak, and T. A. Denidni, "Mutual coupling reduction in millimeter-wave MIMO antenna array using a metamaterial polarization-rotator wall," *IEEE Antennas Wireless Propag. Lett.*, vol. 16, pp. 2324–2327, 2017.
- [23] N. K. Sahu, G. Das, and R. K. Gangwar, "Dielectric resonator-based wide band circularly polarized MIMO antenna with pattern diversity for WLAN applications," *Microw. Opt. Technol. Lett.*, vol. 60, no. 12, pp. 2855–2862, Dec. 2018.
- [24] G. Das, A. Sharma, and R. K. Gangwar, "Dielectric resonator based circularly polarized MIMO antenna with polarization diversity," *Microw. Opt. Technol. Lett.*, vol. 60, no. 3, pp. 685–693, Mar. 2018.
- [25] A. Sharma, G. Das, and R. K. Gangwar, "Dual polarized triple band hybrid MIMO cylindrical dielectric resonator antenna for LTE2500/WLAN/WiMAX applications," *Int. J. RF Microw. Comput. Aided Eng.*, vol. 26, no. 9, pp. 763–772, Nov. 2016.
- [26] M. K. A. Nayan, M. F. Jamlosand, and M. A. Jamlos, "Mimo circular polarization array antenna with dual coupled 90° phased shift for point-to-point application," *Microw. Opt. Technol. Lett.*, vol. 57, no. 4, pp. 809–814, Apr. 2015.
- [27] N. K. Sahu, G. Das, and R. K. Gangwar, "Dual polarized triple-band dielectric resonator based hybrid MIMO antenna for WLAN/WiMAX applications," *Microw. Opt. Technol. Lett.*, vol. 60, no. 4, pp. 1033–1041, Apr. 2018.
- [28] M. Abedian, S. K. A. Rahim, S. Danesh, S. Hakimi, L. Y. Cheong, and M. H. Jamaluddin, "Novel design of compact UWB dielectric resonator antenna with dual-band-rejection characteristics for WiMAX/WLAN bands," *IEEE Antennas Wireless Propag. Lett.*, vol. 14, pp. 245–248, 2015.
- [29] I. Amjad, O. A. Saraereh, A. W. Ahmad, and S. Bashir, "Mutual coupling reduction using F-shaped stubs in UWB-MIMO antenna," *IEEE Access*, vol. 6, pp. 2755–2759, 2018.



USMAN ILLAHI received the B.Sc. degree in electrical engineering from the NWFP University of Engineering and Technology, Peshawar, Pakistan, in 2007, and the M.Sc. degree in electronic communication and computer engineering from The University of Nottingham Malaysia Campus, in 2013. He is currently pursuing the Ph.D. degree in electrical and electronic engineering with Universiti Kuala Lumpur, Malaysia, with a focus on antenna microwave communication systems, especially antennas, such as dielectric resonator antennas, circularly polarized antennas, wideband antennas, and wearable antennas.



MOHAMAD ISMAIL SULAIMAN received the M.Eng. and Ph.D. degrees in electronic engineering (communications) from The University of Sheffield, U.K., in 2007 and 2012, respectively. Since 2013, he has been a Senior Lecturer with the Universiti Kuala Lumpur British Malaysian Institute. He has authored more than 30 research articles published in journals and peer-reviewed conferences. His research interests include computational electromagnetic, dielectric resonator antennas, circularly polarized antennas, wideband antennas, mutual coupling, and wearable antenna.



MUHAMMAD MANSOOR ALAM received the M.E. degree in systems engineering, the M.Sc. degree in computer science, the Ph.D. degree in computer engineering, and the Ph.D. degree in electrical and electronic engineering. He is an Active Researcher in the field of telecommunication and network. He has authored more than 60 research articles published in ISI indexed journals, as book chapters, and in peer reviewed conferences. He has also authored the book *Study Guide of Network Security* copyrighted by Open University Malaysia and The Open University of Hong Kong. He is also an Active Reviewer for the ISI indexed journal *Pertanika Journal of Science and Technology (JST)*.



MAZLIHAM MOHD SU'UD received the Ph.D. degree in computer engineering from the Université de La Rochelle, in 2007, and the master's degree in electrical and electronics engineering from the University of Montpellier, in 1993. Since 2013, he has been the President/CEO of Universiti Kuala Lumpur, Malaysia.



MOHD NAJIB MOHD YASIN received the M.Eng. degree in electronic engineering and the Ph.D. degree from The University of Sheffield, Sheffield, U.K., in 2007 and 2013, respectively. Since 2013, he has been a Lecturer with the School of Microelectronics, Universiti Malaysia Perlis, Malaysia. His research interests include computational electromagnetic, conformal antennas, mutual coupling, wireless power transfer, array design, and dielectric resonator antennas.



JAVED IQBAL received the B.Sc. degree in telecommunication engineering from the NWFP University of Engineering and Technology, Peshawar, Pakistan, in 2007, and the M.Sc. degree in electronic communication and computer engineering from The University of Nottingham Malaysia Campus, in 2013. He is currently pursuing the Ph.D. degree in electrical and electronic engineering with Universiti Kuala Lumpur, Malaysia, with a focus on antenna microwave communication systems, especially antennas, such as dielectric resonator antennas, circularly polarized antennas, wideband antennas, and multiple-input multiple-output (MIMO) antennas.